Paper:

Effectiveness of Small Onshore Seawall in Reducing Forces Induced by Tsunami Bore: Large Scale Experimental Study

Mary Elizabeth Oshnack*, Francisco Aguíñiga, Daniel Cox*, Rakesh Gupta*, and John van de Lindt*****

*Oregon State University, Corvallis, Oregon 97331-3212, USA
E-mail: moshnack@gmail.com, dan.cox@oregonstate.edu
**Texas A&M University-Kingsville, Kingsville, Texas 78363-8203, USA
***Colorado State University, Fort Collins, CO 80523-1372, USA
[Received August 15, 2009; accepted October 29, 2009]

Tsunami force and pressure distributions on a rigid wall fronted by a small seawall were determined experimentally in a large-scale wave flume. Six different seawall heights were examined, two of which were exposed to a range of solitary wave heights. The same experiment was done without a seawall for comparison. The measured wave profile contained incident offshore, incident broken, reflected broken, and transmitted wave heights measured using wire resistance and ultrasonic wave gauges. Small individual seawalls increased reflection of the incoming broken bore front and reduced force on the rigid landward wall. These findings agree well with published field reconnaissance on small seawalls in Thailand that showed a correlation between seawalls and reduced damage on landward structures.

Keywords: tsunami hazard mitigation, tsunami inundation, tsunami risk reduction, tsunami defense strategy, wave forces

1. Introduction and Background

1.1. Significance of This Study

The December 2004 Indian Ocean Tsunami visited tremendous loss of life and severe damage on coastal communities and infrastructure, reminding the world of the vulnerability of such communities and infrastructure in tsunami occurrence. Prior to this disaster, few research groups specifically studied tsunami force and subsequent structural failure modes, and many findings were based on field reconnaissance or small-scale experimentation rather than large-scale testing. While several experiments have been conducted on wave force on vertical walls, most have, again, been small-scale or considered regular or random waves rather than the unique solitary wave form and bore like loading conditions present during tsunamis. The experiments in this study provide large-scale data for tsunami-induced force and pressure on a stiff aluminum wall. As several field studies have found qualitative correlation between the presence of small seawalls and reduced wave energy, this study provides quantitative data for tsunami loading on a rigid wall fronted by a small seawall. This analysis of the effectiveness of small seawalls in reducing wave force is expected to be valuable in helping protect coastal communities vulnerable to tsunamis.

Fig. 1. Small seawall at Patong Beach, Phuket, Thailand (Photo courtesy of Robert Dalrymple).

1.2. Literature Review

Numerous studies have covered generation and propagation of tsunamis through the open ocean; however, research on inundation and tsunami impacts on structures is less common. Wave force on vertical walls has long been studied, but most experiments have been small-scale. Theoretical pressure profiles from water-wave impact on walls have been studied in great detail by Peregrine (2003). Several hydraulic model studies have focused on tsunami loading on structures (Ramsden 1996; Thusyanthan and Madabhushi 2008; Arikawa, 2008). Ramsden (1996) focused on the impact of translatory waves (bores and dry-bed surges) rather than breaking waves on a vertical wall at a small scale, but his instrumentation did not resolve short-duration shock loads, and the measured force and moment should only be used for design related to sliding and overturning failure, and are not applicable to punching failure. Thusyanthan and Madab-

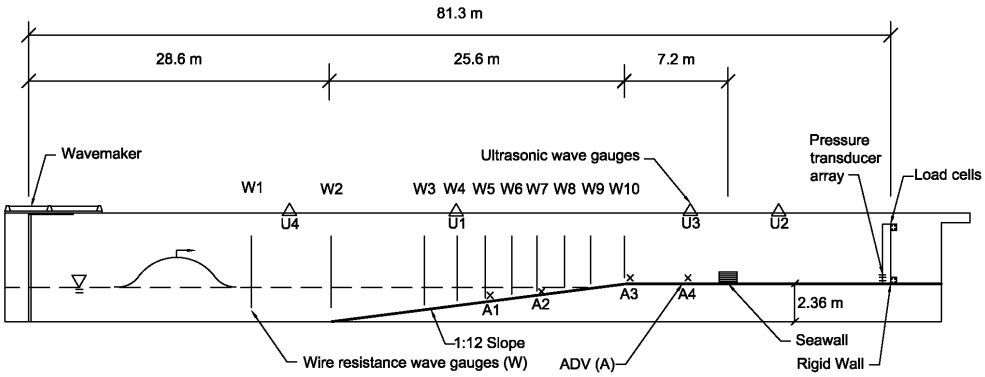

Fig. 2. Elevation of wave flume with experimental setup: *W* is a wire resistance wave gauge, *U* a sonic wave gauge, and *A* an acoustic-Doppler velocimeter.

hushi (2008) studied the effects of appropriate anchoring and increased openings in the front of 1 : 25 scale coastal housing on tsunami force and pressure. Arikawa (2008) showed mechanisms of failure due to impulsive loading by tsunamis on vertical concrete walls using large-scale hydraulic flume tests.

Yeh. et al. (2005) developed design guidelines for buildings subjected to tsunami loading by analyzing tsunami force in detail and compiling equations currently addressing loads under flooding and wave situations from the City and County of Honolulu Building Code (CCH 2003), Uniform Building Code (UBC 1997), International Building Code (IBC 2000), American Society of Civil Engineers Committee 7 (ASCE 2006), and Federal Emergency Management Agency Coastal Construction Manual (FEMA 2000).

In addition to theoretical work and laboratory experiments, field reconnaissance has achieved further understanding of tsunami loading. The performance of buildings in Thailand during the 2004 Indian Ocean Tsunami was reported by Lukkunaprasit and Ruangrassamee (2007), Ruangrassamee et al. (2006), Pomonis et al. (2006), and Saatcioglu et al. (2006). For example, hydrodynamic force from the tsunami was found to be much greater than the previously expected wind based design load for coastal buildings. Poor construction practices and inadequate detailing have contributed to structural failures caused by tsunami loading. Lukkunaprasit and Ruangrassamee (2007) noted that low retaining walls – seawalls 1 m high – effectively dissipated tsunami energy. One such wall at Patong Beach in Phuket, Thailand, caused a high splash-up of the incoming wave that has been documented by tourist videos and photographs. A photograph of this seawall is shown in **Fig. 1**, and buildings directly landward of the seawall suffered only modest structural damage. Dalrymple and Kreibel (2005) suggested that the splash up of the wave deflected part of the wave's momentum skyward, reducing force on landward structures. Conducting more detailed reconnaissance on the chain of seawalls in Phuket, Dalrymple and Keibel (2005) found that increased damage was observed directly behind pedestrian openings in the seawall chain. Thus, there is a correlation between small seawalls and reduced structural damage.

This paper discusses large-scale experiments on tsunami bores impacting a stiff wall fronted by a small seawall. Section 2 outlines the experimental setup, including flume bathymetry, test specimens and seawalls, and instrumentation. Section 3 explains experimental procedures, including data acquisition and processing and the test matrix and experimental processes. Section 4 presents results, including examples of raw data, data reduction, and comparisons of force as a function of tsunami and seawall height. Section 5 discusses findings, and Section 6 summarizes conclusions.

2. Experimental Setup

2.1. Wave Flume Bathymetry

These experiments were conducted in the large wave flume (LWF) at the O.H. Hinsdale Wave Research Laboratory at Oregon State University. The 104 m long, 3.66 m wide, 4.57 m deep flume has a piston wavemaker with a 4 m stroke and a maximum speed of 4 m/s able to generate replicable solitary waves. Beginning at the wavemaker, bathymetry consisted of a 29 m flat section, 26 m of impermeable beach on a 1 : 12 slope, and a horizontal flat section raised on a 2.36 m high false floor called the "reef." As shown in **Fig. 2**, the specimen and seawall were located along the reef, which was 30 m long. Given x-locations are based on the wavemaker board in the zero position. Note the typical still water level (SWL) and that, under these conditions, no water covered the reef.

2.2. Test Specimen and Small Seawall

The specimen to be tested consisted of an aluminum plate and was 2.14 m high and 3.66 m wide – the wave flume width. The aluminum wall was reinforced with ten vertical studs 0.055 m by 0.178 m spaced at 0.393 m (0.350 m on the two ends), and two horizontal studs 0.120 m by 0.205 m. As also shown in **Fig. 2**, the front of the rigid wall was 81.3 m from the zeroed wavemaker.

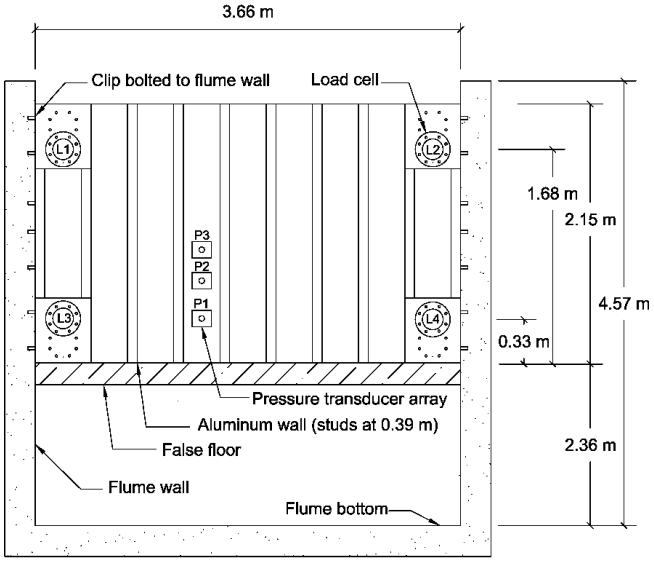

Fig. 3. Elevation of test specimen with instrumentation: *L* denotes load cells and *P* pressure transducers.

Fig. 3 shows overall aluminum wall dimensions and stud locations for the LWF. The small seawall was constructed using dimensional Douglas fir boards 3.8 cm high and 23.5 cm wide stacked vertically and bolted to the flume floor. The seawall was 7.2 m landward of the transition from the reef to the beach and 20 m seaward from the aluminum wall.

2.3. Instrumentation

Ten wire resistance wave gauges and four ultrasonic wave gauges along one side of the flume wall measured variations in instantaneous water surface level. These wave gauges were calibrated at the start of the experiment and when the flume was drained and refilled. From the wavemaker in the zeroed position, wire resistance wave gauges 1 to 10 were located at x-locations of 17.6 m, 28.6 m, 35.9 m, 40.6 m, 42.4 m, 44.2 m, 46.1 m, 48.2 m, 50.3 m, and 54.4 m. Ultrasonic wave gauge 1 was co-located with wave gauge 4 (40.6 m), enabling the calibration of other surface piercing gauges to be corrected for changes due to variation in chlorine from the city water supply. Surface piercing wave gauge accuracy was estimated at less than 1% of the full-scale reading for non-broken waves. A sonic gauge seaward ($x = 58.1$ m) and landward ($x = 65.1$ m) of the small seawall estimated incident, reflected, and transmitted wave heights, detailed later. A sonic wave gauge was also located on the moveable bridge at 21.5 m from the zeroed wavemaker. The wavemaker was instrumented with sensors to monitor its x position and the water level on the wavemaker board as functions of time. Four acoustic Doppler velocimeters (ADVs) on the side of the flume at x-positions of 43.3 m, 47.0 m, 54.2 m, and 57.9 m collected wave particle velocity for comparison to numerical models, presented elsewhere. **Fig. 2** shows the locations of flume instrumentation, where W is a wire resistance wave gauge, U a sonic wave gauge, and A an acoustic-Doppler velocimeter.

Table 1. Experimental trials run during seawall experiment.

Experiment	Trial	D_0	D_R	H	H_2	D_s
	-	[m]	[m]	[m]	[m]	[m]
RigidWall_4	1	2.29	-0.07	0.80	0.74	0.00
	2	2.29	-0.07	1.00	0.90	0.00
	3	2.29	-0.07	1.20	1.09	0.00
	4	2.29	-0.07	1.40	1.24	0.00
	5	2.29	-0.07	1.30	1.15	0.00
	6	2.29	-0.07	1.10	0.96	0.00
	7	2.29	-0.07	0.40	0.39	0.00
Macro_1	1	2.29	-0.07	0.80	0.74	0.24
	2	2.29	-0.07	1.00	0.92	0.24
	3	2.29	-0.07	1.20	1.06	0.24
	4	2.29	-0.07	0.40	0.39	0.24
	5	2.29	-0.07	0.60	0.56	0.24
Macro_2	1	2.29	-0.07	0.40	0.39	0.12
	2	2.29	-0.07	0.60	0.57	0.12
	3	2.29	-0.07	0.80	0.74	0.12
	4	2.29	-0.07	1.00	0.91	0.12
	5	2.29	-0.07	1.20	1.06	0.12
	6	2.29	-0.07	0.80	0.74	0.16
	7	2.29	-0.07	0.80	0.74	0.20
	8	2.29	-0.07	0.80	0.74	0.80
	9	2.29	-0.07	0.80	0.73	0.40

The specimen had four uniaxial donut-shaped load cells with a capacity of $\pm$89 kN ($\pm$20 kip). One load cell was installed on each corner of the aluminum wall between a plate on the aluminum wall and a clip bolted to the flume wall specifically to hold the load cell in place. Load cells measured horizontal force on the wall. The specimen also had three pressure transducers (Druck PDCR-830) set horizontal to aluminum plates, which were placed in small holes cut in the wall. Transducers were at 0.22, 0.51, and 0.92 m heights on the wall. Load cells (L1-4) and pressure transducers (P1-3) are shown in **Fig. 3**.

3. Experimental Procedures

3.1. Data Acquisition and Processing

Data were recorded and stored using National Instruments 64-channel PXI-based real-time data acquisition. Software controlling data acquisition was LabVIEW 8. Hydrodynamic data – free surface displacement and velocity – were collected at a sampling rate of 50 Hz. Force and pressure data were collected at a sampling rate of 1000 Hz.

3.2. Experimental Processes

As shown in **Fig. 2**, experiments were conducted with the reef dry, essentially modeling the dry beach common

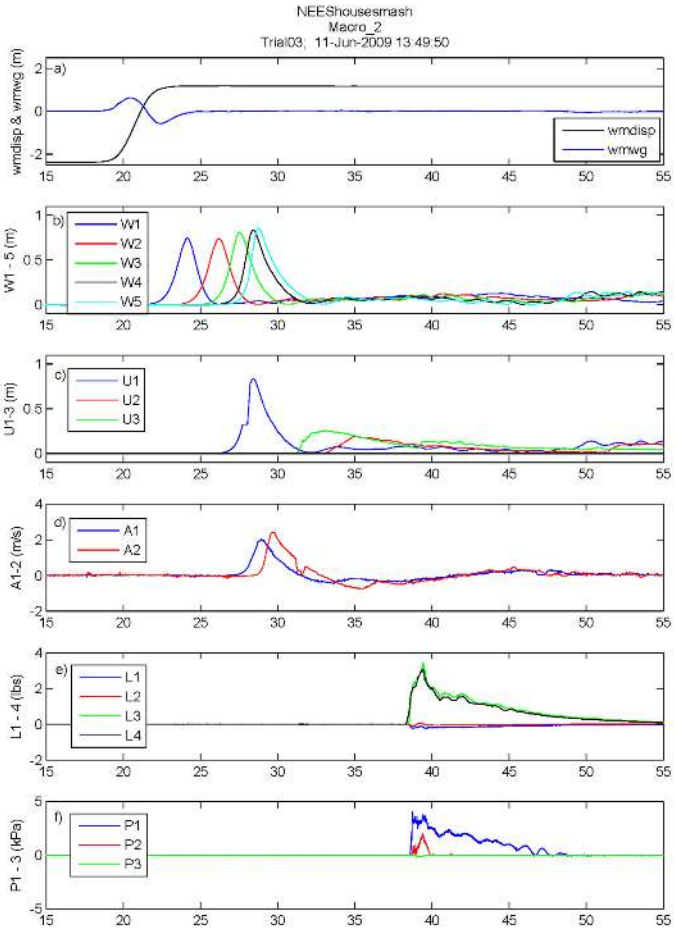

Fig. 4. Example time series of data collected during a typical run corresponding to $H_2 = 0.74$ m ($H = 0.80$ m), $D_s = 0.12$ m: (a) wavemaker displacement and free-surface displacement on the wavemaker; (b) free surface profile: wire resistance wave gauges 1-5; (c) free surface profile: ultrasonic wave gauges; (d) velocity measured by ADV 1, 2; (e) force; and (f) pressure measurements.

at urban waterfronts. While the wavemaker was zeroed, the water level was set at 2.38 m from the flume bottom, at which depth the water level was aligned with the point at which the bathymetry changed from beach to reef. The wavemaker was then fully retracted, decreasing the water level due to the finite flume volume. The still water depth (D_0) with the wavemaker retracted was 2.29 m, corresponding to -0.07 m below the reef (D_R). The tsunami was modeled as an idealized solitary wave using forward paddle movement typical in these studies. Because of the flume's finite volume, this produced a still water level $+0.03$ m above the reef at the end of tests from $40 < t < 55$ s, as can be seen in **Fig. 4(b)**.

Table 1 summarizes the trials. Experiment names and trial numbers correspond to those in the experimental notebook supported under the Network for Earthquake Engineering Simulation (NEES) program of the United States National Science Foundation. The RigidWall_1 experiment is the control group of trials in which force was measured on the aluminum wall with no seawall for protection, Macro_1 is testing of a 0.24 m seawall under a variety of wave heights. Marco_2 is the testing of different seawall heights, detailed below. H is the desired nominal wave height input to the wavemaker, H_2 is the wave height measured by offshore wave gauge 2, D_S is the seawall height and D_0 and D_R the still water and reef depth defined above. Experimental data will be made public through the NEES data archive.

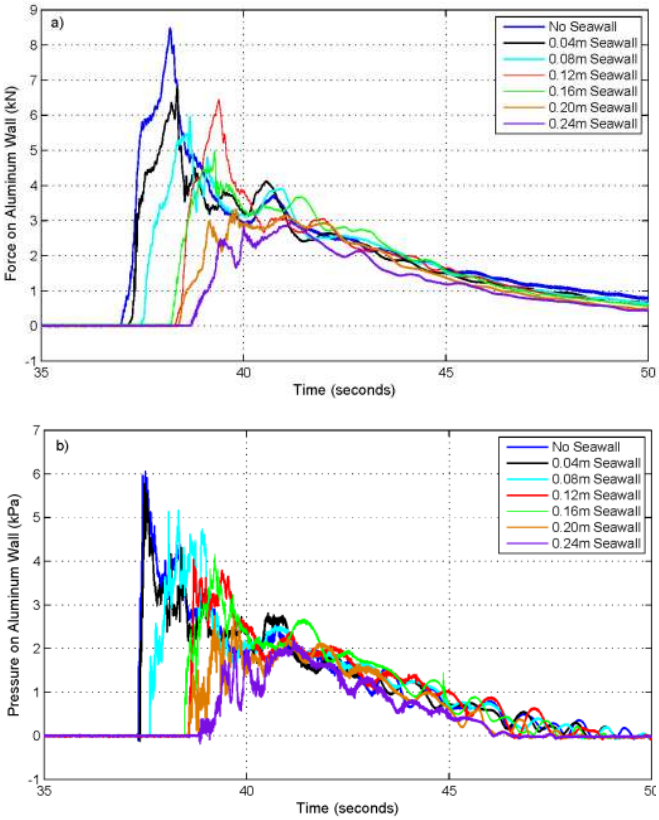

Fig. 5. (a) Total force and (b) pressure time histories for different seawall combinations at a wave height of $H_2 = 0.74$ m ($H = 0.8$ m). Pressure is read from the lowest pressure transducer shown in **Fig. 3**.

Four sets of conditions were run:

Condition 1: A 0.24 m high seawall was placed in the flume as described above. To obtain tsunami force on the specimen under the presence of a 0.24 m seawall as a function of wave height, nominal heights of 0.40, 0.60, 0.80, 1.00, and 1.20 m were run corresponding to heights measured at wage gauge 2 of 0.39, 0.57, 0.74, 0.91, and 1.06 m, as shown in **Table 1**. We refer to the measured wave height at wave gauge 2 and provide the nominal wave height in parentheses for reference to file names in the NEES Experimental Notebook (e.g., Baldock et al., 2008).

Condition 2: The seawall height was changed to 0.12 m and the same waves were run.

Condition 3: To better understand force reduction as a function of seawall height, the height of the wall was changed to 0.04, 0.08, 0.16, and 0.20 m by varying the number of wooden boards composing the wall. A $H_2 = 0.74$ m wave ($H = 0.8$ m) was run for each wall configuration.

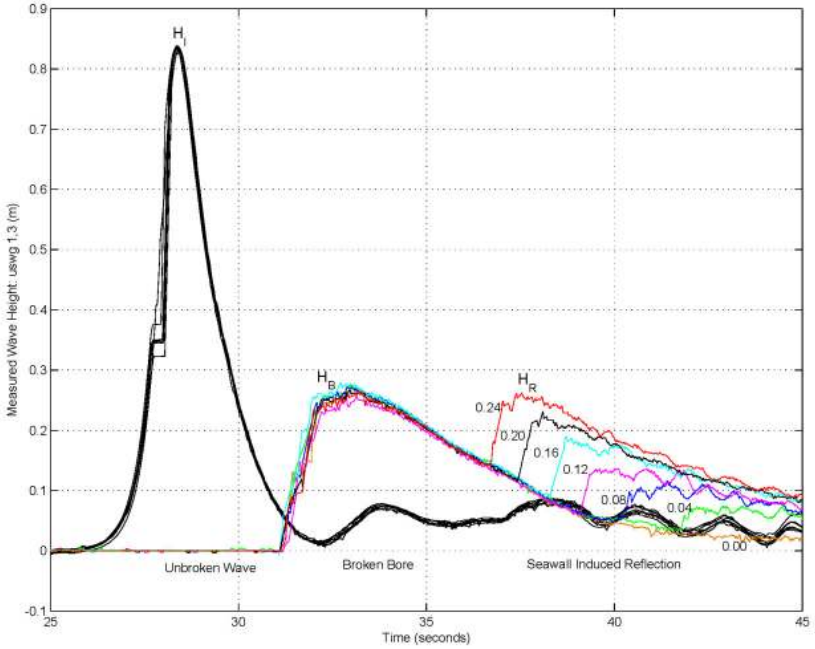

Fig. 6. Free surface time series measured by sonic wave gauges. Numbers in the graph indicated seawall height in meters. Note the high repeatability of measurements shown by the unbroken wave and broken bore. Note the decrease in the reflected bore as seawall height is decreased.

Condition 4: An experiment was conducted under the same conditions with no seawall for comparison. The overall dataset contains 21 runs – 7 with no seawall, 5 with a high 0.24 m seawall, 5 with a low 0.12 m seawall, and 4 additional runs with varied seawall heights under an $H_2 = 0.74$ m ($H = 0.8$ m) wave. The 0.24 m and 0.12 m walls are included in this set of 6 runs for comparison.

4. Results

An example of data collected is shown in **Fig. 4** for an experimental run using a wave height of $H_2 = 0.74$ m ($H = 0.8$ m) and a seawall height of 0.12 m. **Fig. 4** shows the following variables – (4a) wavemaker displacement (black) and free-surface displacement on the wavemaker (blue); (4b) free surface displacement measured by wire resistance wave gauges 1-5 with a total of 10; (4c) free surface displacement collected by ultrasonic wave gauges – incident before breaking (blue – wave gauge 1), transmitted over the seawall (red – wave gauge 2), and broken incident/reflected off the seawall (green – wave gauge 3); (4d) velocity measured by ADV 1 and 2 from a total of 4; (4e) force data collected by the four load cells – L3 and L4 at the bottom of the wall and L1 and L2 at the top; and (4f) pressure data collected by pressure transducers PS 1, PS 2, and PS 3 located at heights of 0.218 m, 0.512 m, and 0.921 m on the wall. Graphs similar to these were made for each run to ensure all instrumentation was operating properly. Note that ADV data were filtered to reduce unwanted noise from air entrainment.

Figure 5 shows force and pressure time histories for each seawall at a wave height of $H_2 = 0.74$ m ($H = 0.8$ m).

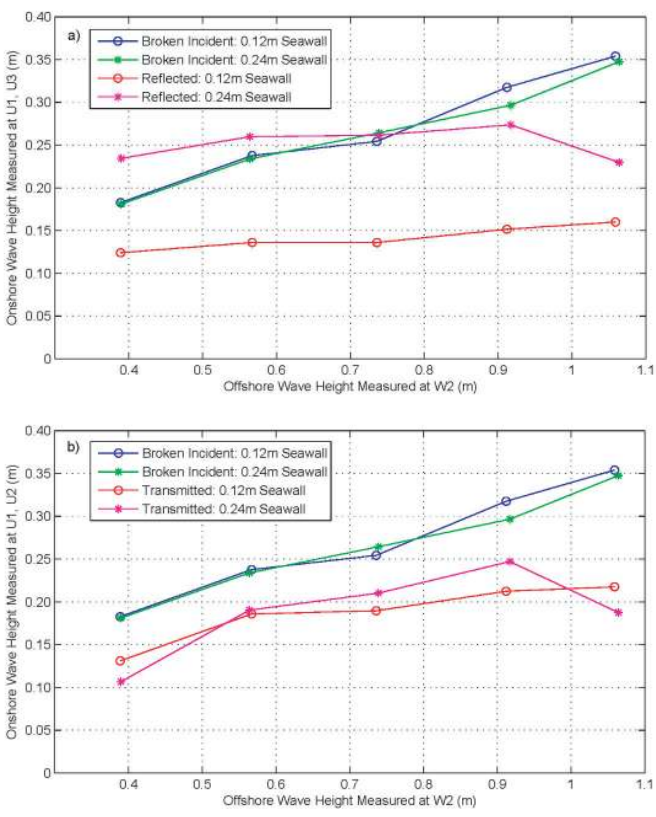

Fig. 7. Reflected bore height measured by ultrasonic wave gauge 3 (a-red, magenta), and transmitted bore heights by ultrasonic wave gauge 2 (b-red, magenta) as functions of offshore wave height measured by resistance wave gauge 2. Both cases of broken incident waves were measured by ultrasonic wave gauge 1 (a, b-blue, green).

Total force on the rigid wall was obtained by summing the four load cells, and the pressure transducer at the lowest elevation, P1, gave the pressure time history. As shown in **Fig. 4(f)** the two pressure transducers higher on the wall had small or, in many cases, zero readings, so the lowest pressure transducer was representative of the depicted pressure time history. Note that as seawall height increases, force and pressure peaks decrease. Comparing the 0.24 m seawall (green) and no seawall (blue) force profile shows that maximum force under a 0.24 m seawall is only 35% of force in the absence of the seawall, which reduces total force by 65%. The graph also shows that the force profiles for the 0.20 m and 0.24 m seawalls are absent of the sharp force peaks that are present under smaller seawall heights. Pressure distributions show similar trends. Note the distinction between relatively smooth integrated force measured by load cells, as shown in **Fig. 5(a)**, and high localized pressure fluctuation shown in **Fig. 5(b)**. Note that as seawall height increases, the time it takes for the wave to impact the wall – determined by the start of the sharp increase or "heel" in the force time history – increases similarly, showing that seawalls act to decrease bore speed. This potentially interesting affect requires further study.

In addition to reduced force, seawalls were also found to cause reflection/splash-up of the broken incoming wave's profile. **Fig. 6** shows the unbroken measured height H_I from sonic wave gauge 1, the height of the broken bore H_B, and the height of the broken bore reflected off of the seawall, H_R (both H_B and H_R were measured by sonic wave gauge 3). As expected, the highest seawall caused the greatest reflection – an H_R/H_B ratio of nearly 1 – and the height of the reflected wave decreases with seawall height over the range of conditions tested. **Fig. 6** also shows the high level of repeatability in wave height measurement. Note the similarity between offshore wave profiles (black lines) even after breaking and the broken bore (colored lines) before hitting the seawall. This high level of repeatability for incident and broken waves lends credibility to reflection measurement. **Fig. 7** shows maximum broken incident (H_B), broken reflected (H_R), and transmitted (H_T) waves for 0.12 and 0.24 m seawalls for a range of wave heights. Broken incident wave conditions are very similar regardless of seawall height, this is also shown in **Fig. 6**, and the height of the broken incident wave increases linearly as offshore wave height H_2, measured by wave gauge 2, increases. Note that for the 0.24 m seawall when H_B is less than the height of the seawall, D_S, reflection exceeds the incident broken wave height. When H_B is nearly equal to D_S, reflection is very close to the incident broken wave height, and when H_B exceeds D_S, reflection is less than the broken incident wave height. For the 0.12 m seawall, H_B is greater than D_S for each wave condition, and reflection is less than the broken incident wave height. **Fig. 7(b)** shows that the transmitted wave height increases linearly with offshore wave height for both seawalls.

Figure 8 summarizes experimental findings showing measured force, pressure, time for the broken bore to reach the aluminum wall, and the ratio of H_R to H_B as functions of seawall height. As expected, the largest seawall causes the lowest force and pressure on the aluminum wall by reflecting the greatest percentage of the broken bore. It also takes the longest for the bore front to reach the rigid wall in the presence of the largest seawall. **Fig. 9** shows a similar trend in plotting maximum force and percent reflection for 0.12 and 0.24 m seawalls at a variety of wave heights. As expected, force increases with wave height and the highest seawall reduces force the most over the range of wave heights tested. A similar trend was found for pressure (not shown due to space limitations). As shown by **Fig. 7** and reaffirmed by **Fig. 9**, the 0.24 m seawall effectively deflected each wave height. The 0.12 m seawall was also effective, especially at lower wave heights.

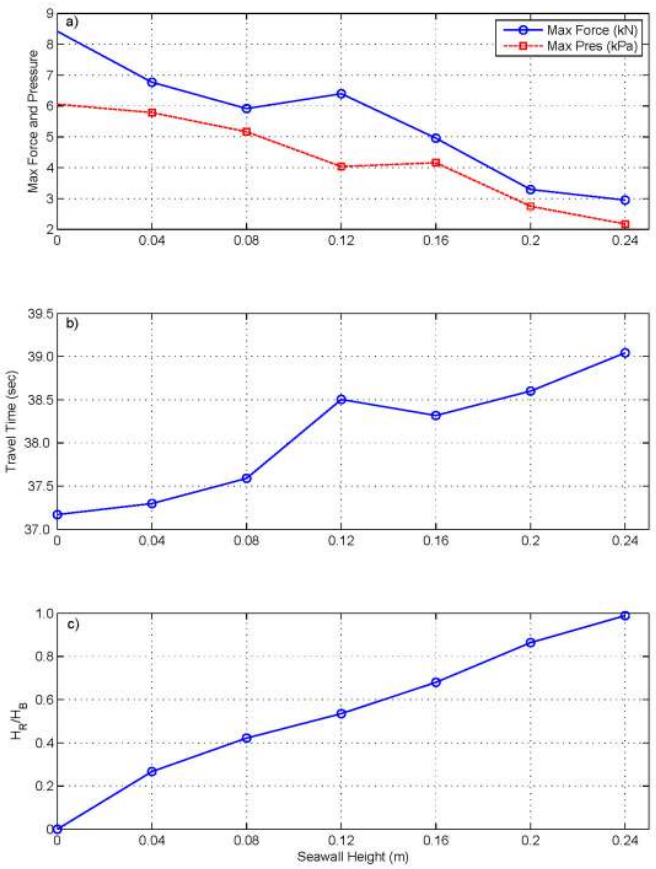

Fig. 8. (a) Force and pressure, (b) travel time, and (c) reflection variations with seawall height for a wave height of $H_2 = 0.74$ m ($H = 0.8$ m).

5. Discussion

Figure 5 suggests that higher seawalls (0.20 and 0.24 m) reduce total force so as to eliminate sharp peaks (impulse loading) for a $H_2 = 0.74$ m ($H = 0.8$ m) wave height. Note that the force profile for the 0.12 m seawall in **Fig. 5** is somewhat peculiar. Other profiles appear to have a group of high force readings before the peak,

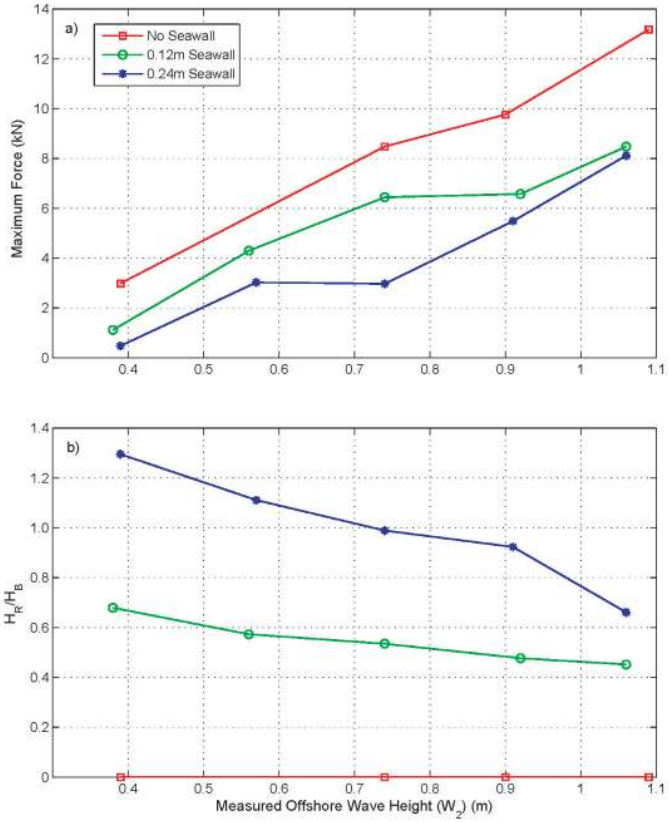

Fig. 9. (a) Maximum force and (b) reflection as a function of measured offshore wave height.

while the force profile in the presence of the 0.12 m seawall (red line) appears to rise rapidly to the peak. This slightly skewed profile explains why travel time for the 0.12 m seawall in **Fig. 8** is slightly above the linear trend shown by other points. Peak force in the presence of a 0.12 m seawall is slightly higher than the peak for a 0.16 m seawall, and the reason for this discrepancy is unknown. Both lower load cells exhibit similar force time histories and replays of the video for this run did not provide any insight. Further experimentation, possibly coupled with numerical investigations, are thus needed to attain conclusive results.

Figure 7 suggests that the maximum reflection height is governed somewhat by seawall height. For both seawall heights, when the height of the broken incident wave exceeded seawall height heights of transmitted and reflected waves were both less than the height of broken incident waves. For the two cases in which the height of the broken incident wave was less than the seawall height, reflected wave height exceeded broken incident wave height. The relationship that can be drawn from **Fig. 7** between waves transmitted by 0.12 and 0.24 m seawalls is somewhat inconclusive. For $H_2 = 0.74$ m ($H = 0.8$ m) and $H_2 = 0.90$ m ($H = 1.0$ m) wave heights the larger seawall actually enables higher transmitted wave height. This may be related to the details of the hydraulic jumps formed at the base of the seawall and the rate at which the energy is dissipated.

6. Summary and Conclusions

This study is a first step in further understanding the effectiveness of small-scale seawalls in reducing tsunami wave force. The 0.20 m and 0.24m seawalls most effectively reduced wave force on the rigid wall over the range of conditions tested. Force and pressure time histories for this wave height do not show sharp peaks, indicating that a seawall may effectively reduce impulsive wave force. A further study is required to understand detailed dynamics. A correlation between seawall height and the ratio of broken incident wave height to reflected wave height was also found. Based on the ratio of broken incident wave height to reflected wave height, the 0.24 m seawall effectively reflected wave height. The 0.12 m seawall was also effective ($H_R/H_B > 0.50$) at smaller wave heights, and H_R/H_B was equal to 0.48 and 0.45 for the largest wave heights of 1.0 and 1.2 m. Using a limited number of wave conditions and seawall configurations we concluded that as seawall height is increased, the reflection of the incoming wave is greater, and force on the onshore structural element is reduced. Force reductions observed in these experiments range from 23% to 84% for offshore waves up to 4 times the seawall height – an observation that holds for both 0.12 and 0.24 m high seawalls over the range of wave heights tested. As suggested by a reviewer, it is important to note that the results of this study are only valid for this particular setup because the distance between the seawall and structure should play a role in determining force on the onshore structural element.

Acknowledgements

This research was supported by the National Science Foundation under Grant No. CMMI-0830378. The tsunami facility is supported in part by the George E. Brown, Jr. Network for Earthquake Engineering Simulation (NEES) Program of the United States National Science Foundation under Award Number CMMI-0402490. We thank the O. H. Hinsdale Wave Research Laboratory staff of Tim Maddux, Melora Park, Jason Killian, Sungwon Shin, Alicia Lyman-Holt, and Adam Ryan for its invaluable support. We hereby acknowledge the work of Milo Clauson of Oregon State University, Francisco Galan of San Jose State University, Manuel Guerra of Texas A&M Kingsville, and Sangki Park of Colorado State University for their assistance in conducting experiments.

References:

[1] T. Arikawa, "Behaviors of concrete walls under impulsive tsunami load," Proc. International Conference on Coastal Engineering, American Society of Civil Engineers, 2008 (in press).
[2] American Society of Civil Engineers (ASCE), "Minimum Design Loads for Buildings and Other Structures," ASCE Standard ASCE 7-06, 2006.
[3] T. E. Baldock, D. Cox, T. Maddux, J. Killian, and L. Fayler, L. "Kinematics of breaking tsunami wavefronts: A data set from large scale laboratory experiments," Coastal Engineering, Vol.56, pp. 506-516, 2008.
[4] CCH 2003 Department of Planning and Permitting of Honolulu Hawaii, "City and County of Honolulu Building Code," Chapter 16 Article 11. July, 2003.
[5] R. A. Dalrymple and D. L. Kriebel, "Lessons in Engineering from the Tsunami in Thailand," The Bridge, National Academy of Engineering, Vol.35, pp. 4-16, 2005.

[6] Federal Emergency Management Agency (FEMA), "Coastal Construction Manual," (FEMA 55), Federal Emergency Management Agency, 2000.
[7] IBC 2003 International Code Council, INC. "International Building Code 2003," Country Club Hills, IL, 2002.
[8] P. Lukkunaprasit and A. Ruangrassamee, "Building Damage in Thailand in the 2004 Indian Ocean Tsunami and Clues for Tsunami-Resistant Design," The IES Journal Part A: Civil and Structural Engineering, Vol.1 No.1, pp. 17-30, 2008.
[9] D. H. Peregrine, "Water-Wave Impact on Walls." Annual Review of Fluid Mechanics," Vol.35, pp. 23-43, 2003.
[10] A. Pomonis, T. Rossetto, N. Peiris, S. Wilkinson, D. Del Re, R. Koo, R. Manlapig, and S. Gallocher, "The Indian Ocean Tsunami of 26 December 2004: Mission Findings in Sri Lanka and Thailand," United Kingdom: Institution of Structural Engineers, 2006.
[11] Ramsden, "Forces on a Vertical Wall Due to Long Waves, Bores, and Dry-Bed Surges," Journal of Waterway, Port, Coastal, and Ocean Engineering, ASCE, Vol.122, No.3, pp. 134-141, May-June 1996.
[12] A. Ruangrassamee, H. Yanagisawa, P. Foytong, P. Lukkunaprasit, S. Koshimura, and F. Imamura, "Investigation of Tsunami-Induced Damage and Fragility of Buildings in Thailand after the December 2004 Indian Ocean Tsunami," Earthquake Spectra, Vol.22, S377-S401, 2006.
[13] M. Saatcioglu, A. Ghobarah, and I. Nistor, "Performance of Structures in Thailand During the December 2004 Great Sumatra Earthquake and Indian Ocean Tsunami," Earthquake Spectra, Vol.22, S355-S375, 2006.
[14] N. I. Thusyanthan and S. P. Madabhushi, "Tsunami Wave Loading on Coastal Houses: a Model Approach," New Civil Engineering International, September 2008, pp. 27-31, 2008.
[15] Uniform Building Code (UBC), "1997 Uniform Building Code," California, 1997.
[16] H. Yeh, I. Robertson, and J. Pruess, "Development of Design Guidelines for Structures that Serve as Tsunami Vertical Evacuation Sites," Washington State Department of Natural Resources, Olympia, WA, 2005.

Name:
Mary Elizabeth Oshnack

Affiliation:
Graduate Research Assistant, Oregon State University

Address:
6300 SW Grand Oaks Dr, Apt C303, Corvallis, OR 97333, USA

Brief Career:
2007- Conducted field reconnaissance in tsunami affected regions of Thailand through Notre Dame's ISTIM program
2008- Obtained B.S. in Civil Engineering with magna cum laude honors from the University of Pittsburgh
2009- Graduate Research Assistant, Hinsdale Wave Research Laboratory at Oregon State University

Selected Publications:
• "Sea Level Rise as a Designed-for Engineering Hazard," with K. Harries, 33rd IAHR 2009 Congress: Water Engineering for a Sustainable Environment, August 9-14, 2009, Vancouver, BC.

Academic Societies & Scientific Organizations:
• Solar Decathlon Team, University of Pittsburgh/Carnegie Mellon University
• Engineers Without Borders, University of Pittsburgh
• American Society of Civil Engineers (ASCE)

Name:
Francisco Aguíñiga

Affiliation:
Assistant Professor, Civil and Architectural Engineering Program, Texas A&M University-Kingsville

Address:
MSC 194; Kingsville, Texas 78363-8203, USA

Brief Career:
1991- B.S. Civil Engineering, Universidad Michoacana (Michoacan, Mexico)
1996- M.S. Civil Engineering, University of Illinois at Urbana-Champaign, Urbana, Illinois
2003- Ph.D. Civil Engineering (Structures), Texas A&M University, College Station, Texas

Selected Publications:
• F. Aguíñiga, K. Matakis, H. Estrada, J. Sai, P. Leelani, and J. Shelden, "Wave Forces on Bridge Decks: State of the Art and State of the Practice Review," Texas A&M University-Kingsville, Report No. FHWA/0-5516-1, 95pp, October 2006.
• F. Aguíñiga, K. Matakis, H. Estrada, J. Sai, P. Leelani, and J. Shelden, "Synthesis of Wave Load Design Methods for Coastal Bridges," Texas A&M University-Kingsville, Report No. FHWA/0-5516-2, 190pp, October 2006.

Academic Societies & Scientific Organizations:
• American Society of Engineering Education (ASEE)

Name:
Daniel Cox

Affiliation:
Professor, School of Civil and Construction Engineering, Oregon State University

Address:
220 Owen Hall, Corvallis, OR 97331, USA

Brief Career:
1995-2002 Assistant Professor, Texas A&M University
2002- Oregon State University.
2002- Director, O.H. Hinsdale Wave Research Laboratory

Selected Publications:
• N. V. Scott, T. J. Hsu, and D. Cox, "Steep Wave, Turbulence, and Sediment Concentration Statistics Beneath a Breaking Wave Field and Their Implications for Sediment Transport," Continental Shelf Research, 2009 (accepted).
• T. Baldock, D. Cox, T. Maddux, J. Killian, and L. Fayler, "Kinematics of Breaking Tsunami Wavefronts: A Data Set from Large Scale Laboratory Experiments," Coastal Engineering, Vol.56, No.5, pp. 506-516, 2009.

Academic Societies & Scientific Organizations:
• American Society of Civil Engineers
• Coastal Ocean Ports River Institute

Name:
Rakesh Gupta

Affiliation:
Professor, Department of Wood Science and Engineering, Oregon State University

Address:
114 Richardson Hall, Corvallis, OR 97331, USA

Brief Career:
1991- Joined Oregon State University
1999- Visiting Scientist, Division of Building, Construction and Engineering, CSIRO, Australia
1998- Research Engineer, Alpine Engineered Products, Inc., Haines City, Florida

Selected Publications:
• J. Wilson, R. Gupta, J. van de Lindt, M. Clauson, and R. Garcia, "Behavior of a One-Sixth Scale Wood-Framed Residential Structure under Wave Loading," J. of Performance of Constructed Facilities, Vol.23, No.5, pp. 336-345, 2009.
• J. van de Lindt, R. Gupta, R. Garcia, and J. Wilson, "Tsunami Bore Forces on a Compliant Residential Building Model," Engineering Structures, Vol.31, pp. 2534-2539, 2009.

Academic Societies & Scientific Organizations:
• American Society of Civil Engineers
• Forest Products Society
• Society of Wood Science and Technology

Name:
John W. van de Lindt

Affiliation:
Professor, Colorado State University

Address:
Civil Engineering Department, Fort Collins, Colorado 80523-1372, USA

Brief Career:
2000- Michigan Technological University
2004- Colorado State University

Selected Publications:
• J. W. van de Lindt and M. Taggart, "Fragility Analysis Framework for Performance-Based Analysis of Wood Frame Buildings for Flood," ASCE Natural Hazards Review, Vol.10, No.3, pp. 113-123, 2009.
• J. W. van de Lindt, Y. Li, W. M. Bulleit, R. Gupta, and P. I. Morris, "The Next Step for ASCE 16 : Performance-Based Design of Wood Structures," ASCE Journal of Structural Engineering, Vol.135, No.6, pp. 611-618, 2009.

Academic Societies & Scientific Organizations:
• Academic Societies & Scientific Organizations: American Society of Civil Engineers (ASCE)
• Associate Editor for Wood, Journal of Structural Engineering (EERI)
• Earthquake Engineering Research Institute